13 mars 1996

IPNO-DRE-96-04

Dynamical effects and IMF production in peripheral and semi-central collisions of Xe+Sn at 50 MeV/nucleon

J.LUKASIK, J.F.LECOLLEY, V.METIVIER, E.PLAGNOL,
B.TAMAIN, G.AUGER, C.O.BACRI, J.BENLLIURE,
B.BORDERIE, and the INDRA collaboration

Contribution to the XXXIV Int. Winter Meeting on Nuclear Physics, Bormio (Italie), 22-27 janvier 1996

Dynamical Effects and IMF Production in Peripheral and Semi-central Collisions of Xe+Sn at 50 MeV/nucleon ⋆

J. Łukasik [a,1], J.F. Lecolley [b], V. Métivier [b,2], E. Plagnol [a], B. Tamain [b], G. Auger [c], Ch.O. Bacri [a], J. Benlliure [c], B. Borderie [a], R. Bougault [b], R. Brou [b], J.L. Charvet [d], A. Chbihi [c], J. Colin [b], D. Cussol [b], R. Dayras [d], E. De Filippo [d], A. Demeyer [e], D. Durand [b], P. Ecomard [c], P. Eudes [f], D. Gourio [f], D. Guinet [e], R. Laforest [b], P. Lautesse [e], J.L. Laville [f], L. Lebreton [e], A. Le Fèvre [c], T. Lefort [b], R. Legrain [d], O. Lopez [b], M. Louvel [b], N. Marie [c], L. Nalpas [d], A. Ouatizerga [a], M. Parlog [a,3], J. Péter [b], A. Rahmani [f], T. Reposeur [f], M.F. Rivet [a], E. Rosato [b], F. Saint-Laurent [c], M. Squalli [a], J.C. Steckmeyer [b], L. Tassan-Got [a], E. Vient [b], C. Volant [d] and J.P. Wieleczko [c].

[a] *Institut de Physique Nucléaire, IN2P3-CNRS, 91406 Orsay Cedex, France*

[b] *LPC, IN2P3-CNRS, ISMRA et Université, 14050 Caen Cedex, France*

[c] *GANIL, CEA, IN2P3-CNRS, B.P. 5027, 14021 Caen Cedex, France*

[d] *CEA, DAPNIA/SPhN, CEN Saclay, 91191 Gif sur Yvette Cedex, France*

[e] *IPN Lyon, IN2P3-CNRS et Université, 69622 Villeurbanne Cedex, France*

[f] *SUBATECH, IN2P3-CNRS et Université, 44072 Nantes Cedex 03, France*

Experimental data obtained with the 4π multidetector system INDRA were used to study the intermediate mass fragment (IMF, $Z \geq 3$) production in peripheral and semi-central collisions of Xe and Sn at 50 MeV/nucleon. It is found that a large fraction of the IMF's detected originates from the midrapidity region. They are supposed to result either from a fast sequential decay or from a neck emission. The size of this effect as well as the competition between the projectile evaporation and "midrapidity" emission are presented as a function of the transverse energy of Z=1 and Z=2 particles. This observable was used as an impact parameter selector.

⋆ Experiment performed at GANIL

[1] permanent address: *Institute of Nuclear Physics, ul. Radzikowskiego 152, 31-342 Kraków, Poland*

[2] present address: *SUBATECH, IN2P3-CNRS et Université, 44072 Nantes Cedex 03, France*

[3] permanent address: *Institute of Physics and Nuclear Engineering, IFA, P.O. Box MG6, Bucharest, Roumania*

1 Introduction

The understanding of the dynamical effects which lead to dissipation of energy in heavy ion collisions in the intermediate energy range (20–100 MeV/nucleon) has been a goal of many works because they reflect intrinsic properties of nuclear matter. From recent experimental studies [1–5] which are in agreement with theoretical calculations [6], it turns out that, for most collisions (from peripheral to almost central), the mechanisms are mainly binary. This feature can be compared with the corresponding behaviour at lower and higher bombarding energies. Below 10 MeV/nucleon binary processes, deep inelastic collisions (DIC), are indeed widely observed, mainly for heavy systems. The reaction is purely binary in the sense that it leads to two excited outgoing products which deexcite by sequential binary decays. In relativistic heavy ion collisions a third emitting source is observed, which is labeled a "participant zone". Of course one may expect a continuous evolution from a pure two source DIC picture to this three source picture, when the bombarding energy evolves in the intermediate energy range. However the nature of this transition has never been studied.

The advent of large acceptance detectors has produced a wide body of data on the deviation from the purely binary picture. Several studies [7,8] have shown that, from 12 MeV/nucleon, fission events for a medium size system point to a very fast process where the fission products are often aligned along the deflection axis and are not isotropically distributed as they should if long fission lifetimes were assumed. For higher energies and various systems, a number of groups [9–14] have shown that, for peripheral reactions, part of IMF's comes from the region in velocity space that could imply the formation of a "neck" which after the interaction phase would either stick to one of the projectile or target remnants and induce some subsequent fast emission, or separate from both and subsequently decay. From these observations, several important questions can be put forward: what, for a given system, is the importance (probability, size, ...) of this effect as a function of the impact parameter, what are its implications on the assumed dissipative mechanisms and how does these features influence our understanding of the production of the IMF's?

The first set of data obtained with INDRA on symmetric, medium size systems (Xe+Sn from 25 to 50 MeV/nucleon) which can favour the above mentioned dynamical effects, can be used to shed some light on this problem [15]. This short contribution will show that the qualities of INDRA can be used to give a quantitative description of these effects as well as study them as a function of an impact parameter. We focus here on the 50 MeV/nucleon bombarding energy.

2 Impact parameter selector

It is a well known fact, illustrated by dynamical calculations, that the reaction mechanism (i.e. dissipation, spin, mass and charge transfer, ...) is very dependent on the impact parameter of the collision. Even with sophisticated 4π devices the impact parameter cannot be directly measured and an event selector, based on observed

quantities, has to be defined and adapted to the detector setup. One of the properties of the INDRA detector [17] is its high efficiency (about 90%) for light charged particles (LCP, Z=1,2), independently of the type of the reaction mechanism involved and hence of the impact parameter. Here we used as a sorting parameter the laboratory transverse energy, Etrans12, of LCP. An advantage of this method is that it gets rid of efficiency problems for peripheral collisions for which the projectile-like or target-like fragments can be undetected due to the energy threshold (target-like) or angular efficiency (projectile-like) effects. Etrans12 may hence be used to sort all the events registered by INDRA, without any a-priori selection.

In Fig. 1, we present some features of Etrans12. The upper left panel presents a

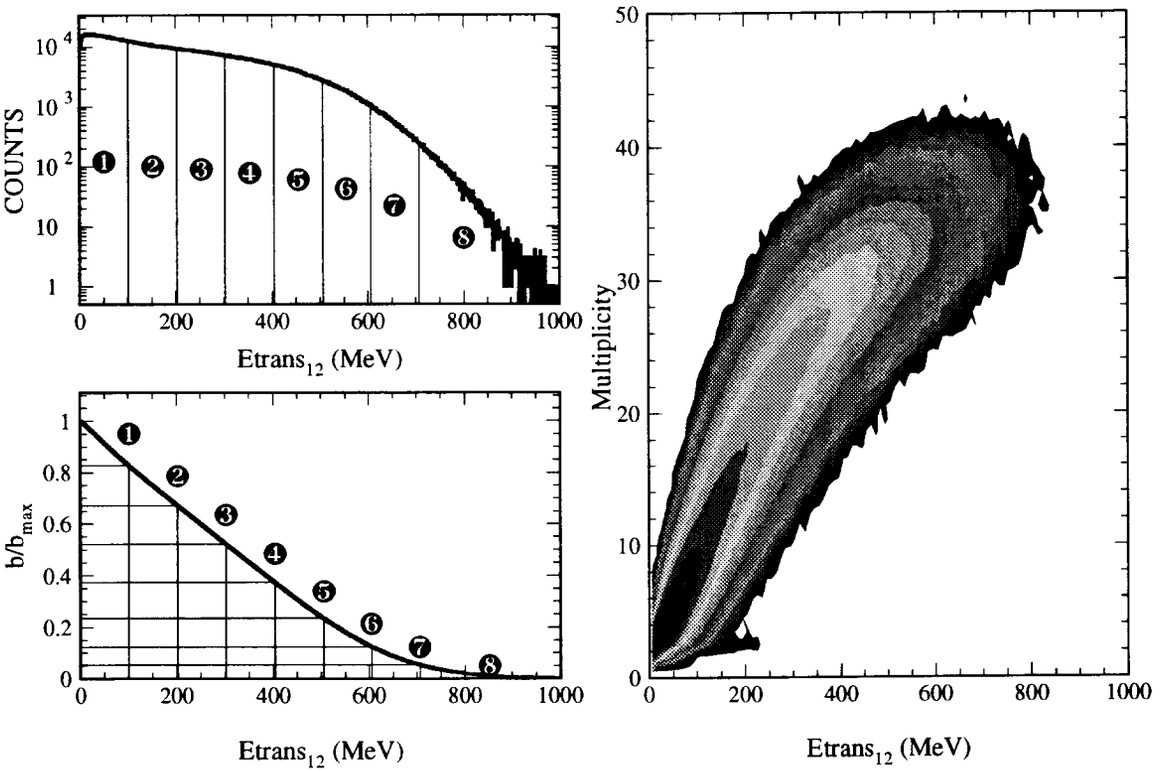

Fig. 1. Upper left panel: the spectrum of the transverse energy of Z=1 and Z=2 particles (Etrans12); lower left panel: the relation between the reduced impact parameter and Etrans12; right panel: the correlation between the multiplicity of charged particles and fragments and Etrans12. The numbers associated with the Etrans12 bins (or the impact parameter bins) are used to identify these bins in the following presentation.

distribution of this observable. This spectrum was divided into 8 bins. The lower left panel presents the relation between Etrans12 and the reduced impact parameter, b/b_{max}, obtained with the use of the geometrical prescription [18]. The maximal impact parameter b_{max} is determined by an experimental trigger and thus refers to the events with at least 4 particles or fragments detected. The last bin corresponds to 5% of the maximal reduced impact parameter. Nevertheless, in this contribution we concentrate on the peripheral and semi-central collisions (bins 1 to 4–5) which exhaust about 80–90% of the total reaction cross section. The right panel of Fig. 1, presents the correlation between Etrans12 and the total multiplicity of charged fragments. The following results are presented as a function of the bin numbers defined in the left part of the figure.

3 Velocity distributions: a signature for slow and fast emissions

In order to have an overall view of the kinematical properties of emitted particles and fragments, it is quite useful to plot the corresponding invariant cross section contours $\frac{d^2\sigma}{v_\perp dv_\perp dv_\parallel}$ in a $v_\perp$ vs $v_\parallel$ plot.

In Fig. 2 such plots, in the center of mass (CM) reference frame, are shown for protons and α particles and for several Etrans12 bins. The binary source behaviour is easily

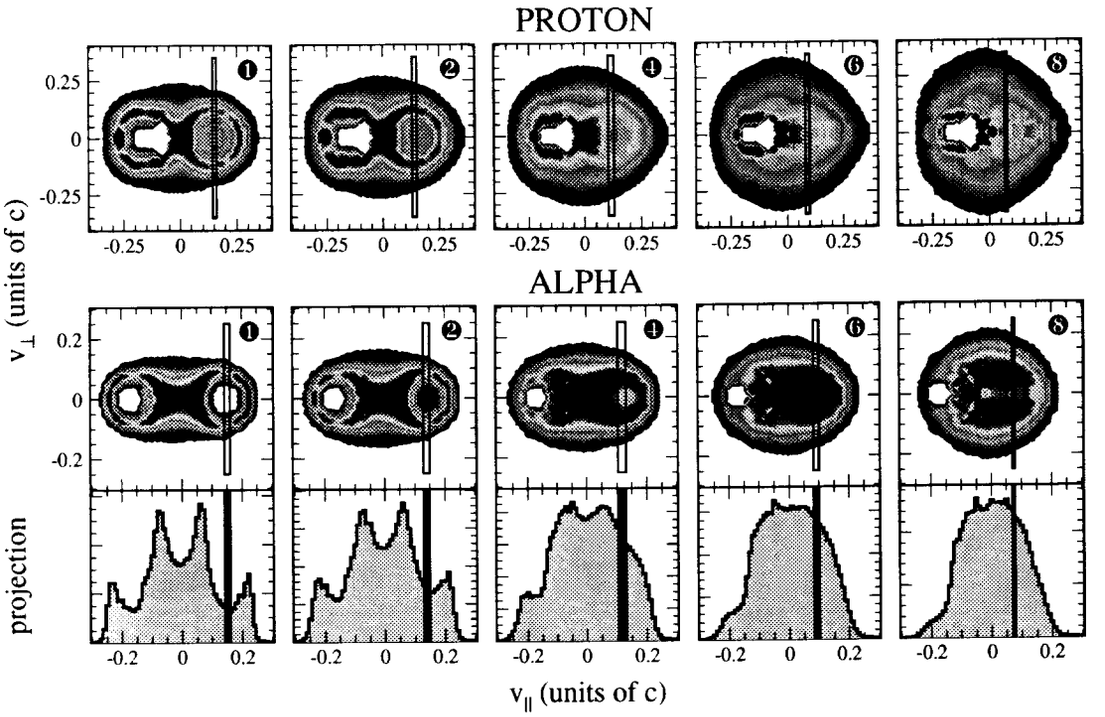

Fig. 2. Invariant velocity plots for protons (upper row) and alpha particles (lower row) detected for specified Etrans12 bins. The right and left sides of the rectangles superimposed on the velocity plots correspond to the source velocities obtained with the use of method I and II, respectively (see text). The presented projections refer to alpha particle plots.

recognized for bins 1–4. For more violent collisions, the separation between the two sources is not so clear and the last bin can correspond to fusion-like events. Now, an interesting observation can be drawn from the figure: when two sources are clearly resolved, all alpha particles cannot be attributed to a statistical sequential decay. Instead, a larger abundance of particles is observed in between the two sources (see also [14]). This "excess" emission can be understood in at least two ways: in the first scenario, a third zone is present, and is responsible for the so-called "neck" emission, which is reminiscent of the participant zone observed at high energies; in the second scenario, these particles are sequentially emitted from one of the outgoing partners, but on a time scale short enough to induce some memory effects in the emission: this second contribution can be referred to as "fast-sequential". The two mechanisms probably contribute to the observed "excess" emission and there is a continuous evolution between them. In both cases, the binary system is dynamically strongly deformed, the "neck" region being either released (neck emission) or attached to one of the outgoing partners, which is hence deformed beyond a pseudo-saddle-point

It is quite useful to quantify the importance of these fast emissions by measuring

leading to a fast break-up. The memory of the partner direction is kept if the emission time is smaller than a few times 10^{-22} s, for an angular momentum in the range 50–100 $\hbar$. A kinematical difference between these two processes can be found in velocity distributions relatively to the main sources. In the case of a pure "neck" emission (two main sources + neck), the corresponding products are likely to be at rest in the CM

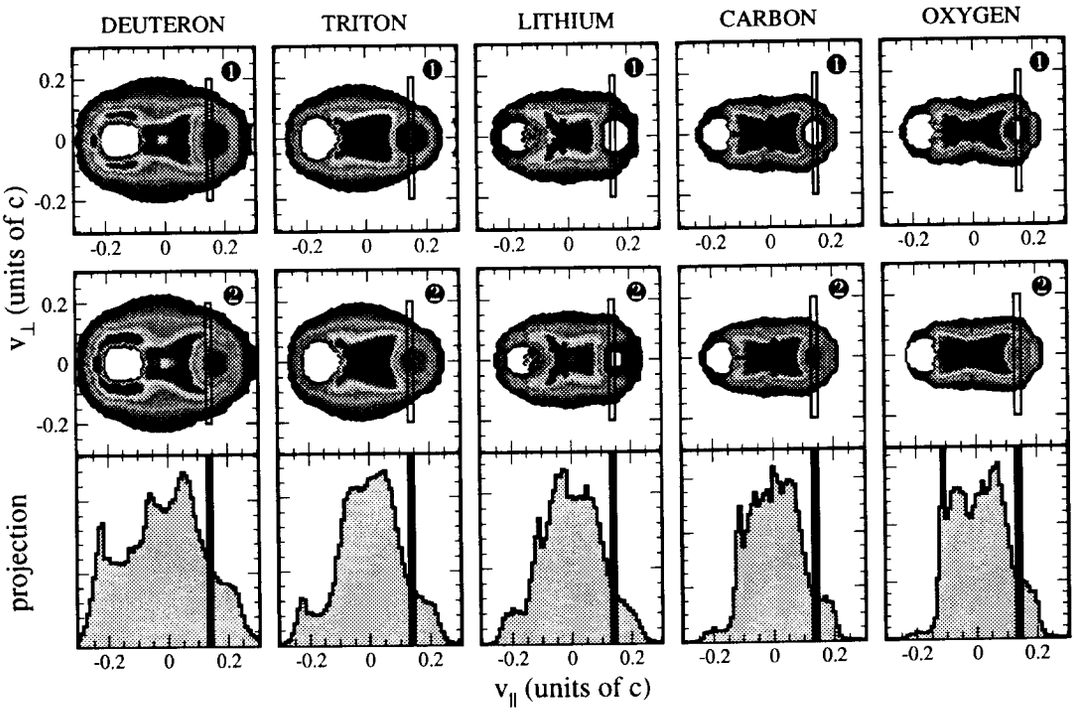

Fig. 3. Invariant velocity plots in the CM frame for deuteron, triton, lithium, carbon and oxygen fragments detected in the most peripheral collisions (upper row – bin 1, and lower row – bin 2 of Etrans12). The right and left sides of the rectangles correspond to the source velocities obtained with the use of method I and II, respectively (see text). The presented projections refer to the plots for the second bin.

frame. Such a contribution can be observed in Fig. 3 for several IMF's. In the case of fast sequential emission, the relative kinetic energy between the detected fragment and its emission source is dominated by the corresponding Coulomb energy. Such a behaviour is observed in Fig. 2 for α particles. It has also been clearly recognized in three-body events [7–10,15].

Since both, neck and fast-sequential, scenarios refer supposingly to the early, dynamical, phase of the reaction and they manifest themselves by relatively low velocity (in the CM) products, they are referred to as "fast" component or "midrapidity" component in this contribution.

4 Quantitative results

It is quite useful to quantify the importance of these fast emissions by measuring the charge percentage which corresponds to neck or fast-sequential decays. For this purpose, one has to estimate the velocities of the two main sources, and to subtract the

component which can be attributed to a sequential decay after complete equilibrium, and which is expected to lead to a forward-backward symmetrical emission in the source frame. The difficulty is to determine properly the velocities of the two main sources.

We performed all the analysis on the quasi-projectile side (positive CM velocities) for which detection efficiency was the best. Since the system is almost symmetric, the results can be easily extrapolated to the whole system. For the peripheral events (bins 1–4) for which the total charge detected is greater than that of the projectile, the heaviest fragment on the projectile side can be regarded as a projectile-like source (PLS). We have tested for each Etrans12 bin, that the most probable velocities of these heaviest fragments are coherent with apparent centers of the Coulomb rings observed in Figs 2 and 3 for LCP's and IMF's. This observation can justify the assignment of these values of velocities to the PLS. However, it is necessary to stress, that this method may lead to an overestimation, since the fast sequential decay exhibits an angular anisotropy, the heaviest fragment is generally pushed in the forward direction in the PLS frame. Similarly, the anisotropy of alpha or IMF emission (Figs 2 and 3) induces a shift of the invariant cross section isocontours.

For these reasons, besides the above method (labeled "method I" later on), we also utilized another method based on the thrust analysis [16] ("method II") to extract the projectile- and target-like fragment velocities. This method is well suited for complete events, for which the whole available charge has been detected. We extend it to events for which the target-like residue has not been detected, but reconstructed from mass and momentum conservation laws. In the thrust analysis, one looks for the best way of attributing all the fragments ($Z \geq 3$) of an event to two sources by maximizing the quantity:

$$T = \frac{|\sum \vec{p}_i| + |\sum \vec{p}_j|}{\sum |\vec{p}_k|}$$

In the numerator, each summation includes fragments which have been attributed to a definite source. The denominator is simply a scaling factor. This method is fully correct if only two sources are involved in the selected events. It leads to underestimated values for the quasi-projectile source if some neck emission occurs, since neck particles are included in the sharing between the two main sources.

Thus in the following analysis we utilize both the above methods and treat them as two extremes. The right and left sides of the rectangles superimposed on the velocity plots in Figs. 2 and 3 correspond to the source velocities obtained with the use of method I and II, respectively.

Having defined the source velocities, it is now possible to estimate the size of the midrapidity (fast) component. It was done by doubling the yield of particles and fragments with velocities greater than the PLS velocity and subtracting it from the total yield in the forward CM hemisphere.

The results are visualized in Fig. 4. Left part of this figure presents the percentage of

charge coming from "neck" and fast-sequential emission – the shaded area bounded by square symbols, and the percentage of charge coming from statistical emission – the shaded area bounded by circles. The filled and open symbols correspond to method I and II, respectively. The width of the bands reflects the sensitivity of the method of measuring the size of the fast component on the source velocity. As can be seen, the percentage of dynamically emitted charge reaches from 12 to 25%, depending on the assumption used to calculate the PLS velocity. Thus it represents a sizable fraction of LCP's and IMF's emitted during the collision. It should be stressed however, that the results above the bins 4–5 should be taken with some care (and in particular the existence of the maximum in the midrapidity/total ratio), since they present the results of extrapolation of the subtraction method above the range of its applicability. The right panels of Fig. 4 answer the question concerning the

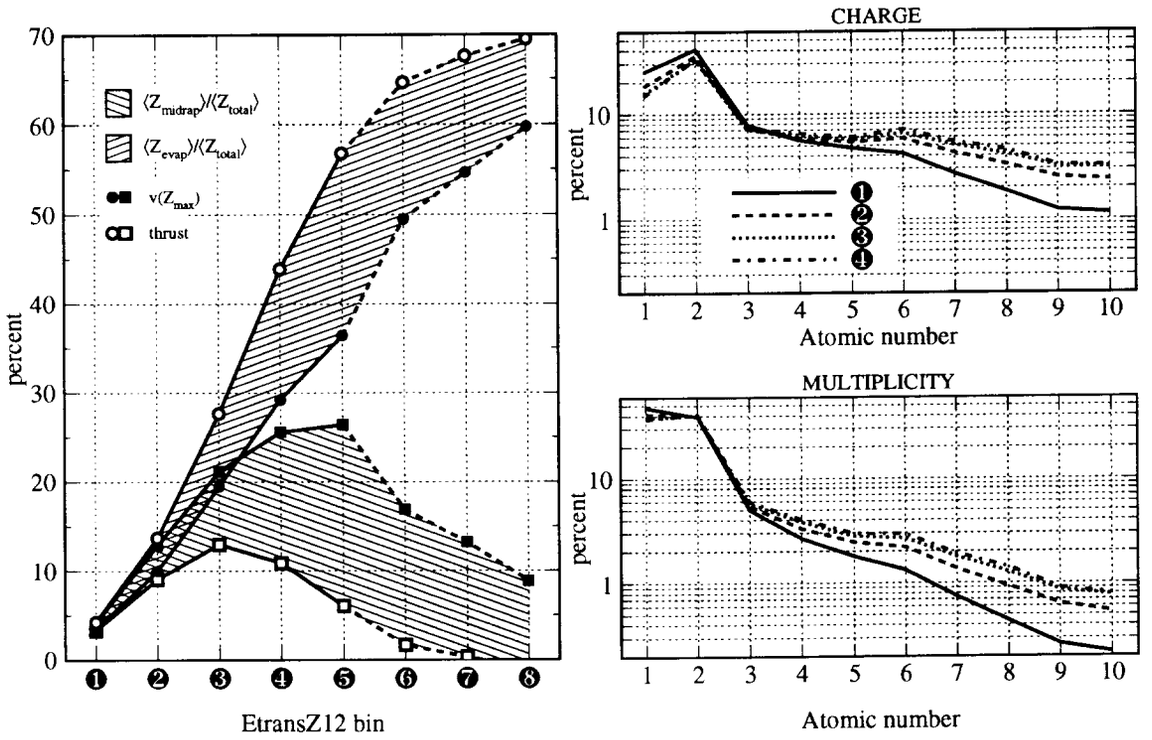

Fig. 4. Left panel: the percentage of charge contained in the midrapidity (fast) component (neck + fast-sequential) – the shaded area bounded by squares; and the percentage of charge coming from statistical emission – the shaded area bounded by circles. The filled and open symbols correspond to method I and II, respectively. Upper right panel: the percentage of charge in the fast component coming from the fragments of a given Z number (Z from 1 to 10) for the Etrans12 bins 1 to 4. Lower right panel: same, but for the multiplicity.

composition of the "neck" and fast-sequential component. The four lines correspond to the Etrans12 bins 1 to 4 and they represent the contribution of fragments with a given Z number to the charge (upper panel) and multiplicity (lower panel) of the fast component. As can be seen from the upper panel the charge of the fast emitted particles comes mainly from LCP's (30–40% from helium isotopes, and 15–25% from hydrogen isotopes), the rest of the charge (35–55%) comes from the IMF's. In the case of multiplicities these contributions are respectively, 40% for helium isotopes, 35–45% for hydrogen isotopes and 15–25% for IMF's. Thus the fast component consists mainly of LCP's, but IMF's represent a sizable fraction of charge and multiplicity,

and their importance increases with the increasing centrality of the collisions.

The above signatures of strong dynamical phenomena are also clearly seen in Fig. 5 in which the lower row presents, for 5 Etrans12 bins, the mean percentage of various particles or fragments, which are attributed to fast component in the method I and II (filled, and open squares, respectively). As can be seen up to 70–85% of light IMF's

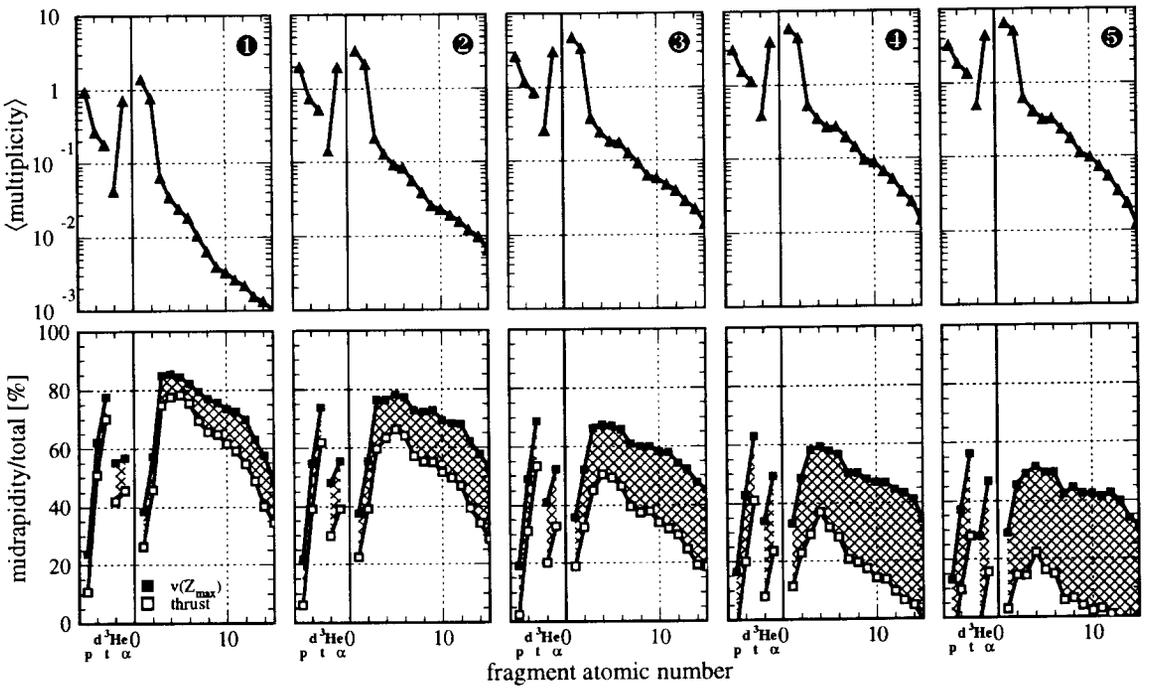

Fig. 5. Upper row: the mean multiplicities of p, d, t, ^{3}He, α and fragments with Z$\leq$15 detected in the forward CM hemisphere for the first 5 Etrans12 bins. Lower row: contribution of the specified above fragments to the fast component. The filled, and open squares correspond to the method I and II, respectively.

($3\leq Z\leq 6$) detected originate from the midrapidity region. Also a very large fraction of tritons (70–80%) come from this zone, what may indicate that the midrapidity emission systematically favours the neutron rich isotopes. The upper row of this figure presents the mean multiplicities per event in the forward CM hemisphere for various LCP's and IMF's. It indicates the relative contributions of the emission of various products. If one integrates the multiplicity distribution for IMF's and takes into account the fast component, one ends up with 1 to 2 IMF's emitted dynamically per event for bins 2–4 (after extrapolating the value to the whole, i.e. projectile + target, system). This value is greater than or comparable with the mean number of statistically emitted IMF's in this region of impact parameters. Thus the "neck" or fast-sequential emission of IMF's in peripheral and semi-central collisions for the system under consideration is not at all an exotic process, moreover, it seems to represent the main source of IMF's for the impact parameters considered.

5 Summary and conclusions

The presented analysis (valid for about 80–90% of the total cross section) indicates that dynamical effects are quite important in peripheral and intermediate impact parameter collisions at 50 MeV/nucleon.

In a simplified picture one can distinguish two "non-statistical" components
– neck (d, t, IMF)
– fast and directed emission from the projectile and the target-like sources (α, fission).

The non-statistical emission can represent up to 12–25% of the total charge for at least 50% of the reaction cross section.

Up to 50–80% of IMF's detected originate from the intermediate velocity region.

The nature of this non-statistical emission is certainly connected with the collective behaviour, since mostly alpha particles and IMF's are involved. In that sense, it differs from the usual preequilibrium mechanism which reflects mainly nucleon-nucleon collisions. A better understanding will require extension of studies to other energies, to symmetrical systems of different size and to assymetrical systems. The data accumulated by the INDRA collaboration will allow to do so.

Other important questions related to these observations are i) the energy (mechanical, thermal, ...) necessary for this fast emission, and the fraction it represents as compared to the excitation energy of the PLS and TLS; ii) the understanding of the nature of this emission and more precisely its connection to the size distribution of the corresponding products; and iii) the influence of the viscosity on the deformation of PLS (TLS) and on the neck formation.

The correct reproduction of all the observed features will imply strong constraints on dynamical models and may be a key requirement before applying them to the multifragmentation data observed in more central collisions [15]. The presented experimental results offer a unique opportunity and challenge for the dynamical models, since they refer to the early phase of the reaction, and thus do not require any "afterburners".

Acknowledgement

J.L. would like to thank the INDRA Group from IPN Orsay for their very warm hospitality, he also acknowledges the Ministère de l'Enseignement Su-

périeur et de la Recherche for the financial support.

References

[1] B. Borderie *et al.*, Phys. Lett. **B205** (1988) 26,
M.F Rivet *et al.*, Proc. of Intern. Wint. Meet. on Nucl. Phys., 1993, p92.

[2] J. Péter *et al.*, Nucl. Phys. **A593** (1995) 95.

[3] J.C. Steckmeyer *et al.*, Preprint LPCC 95–13.

[4] R. Bougault *et al.*, Nucl. Phys. **A587** (1995) 499.

[5] V. Métivier *et al.*, Proc. of the ACS Nucl. Chem. Symp., Anaherm, CA, April 1995.

[6] M. Colonna *et al.*, Prog. Part. Nucl. Phys. **30** (1992) 17,
L. Sobotka, Phys. Rev. **C50** (1994) R1270,
M.F. Rivet *et al.*, Phys. Lett. **B215** (1988) 55,
F. Haddad *et al.*, Preprint Subatech 95–14, submitted to Z. Phys.

[7] P. Glässel *et al.*, Z. Phys **A310** (1983) 185.

[8] G. Casini *et al.*, Phys. Rev. Lett. **71** (1993) 2567.

[9] L. Stuttgé *et al.*, Nucl. Phys. **A539** (1992) 511.

[10] J.F. Lecolley *et al.*, Phys. Lett. **B354** (1995) 202.

[11] C.P. Montoya *et al.* Phys. Rev. Lett. **73** (1994) 3070.

[12] J. Tõke *et al.*, Phys. Rev. Lett. **75** (1995) 2920 – Nucl. Phys. **A583** (1995) 519c.

[13] W. Lynch, Nucl. Phys. **A583** (1995) 471c.

[14] V. Métivier *et al.*, to be published – V. Métivier, thesis Caen (1995).

[15] Indra collaboration: to be published.

[16] J. Pouthas *et al.*, Nucl. Instr. Meth. **A357** (1995) 418.

[17] M.B. Tsang *et al.* Phys. Rev. Lett. **71** (1993) 1502.